A Heuristic-Based Method for Setting Synchronous Distributed Generators Excitation System Parameters to Improve Islanding Detection

Rodrigo de Barros Iscuissati
Moisés Junior Batista Borges Davi
José Carlos Melo Vieira
Department of Electrical and Computer Engineering
São Carlos School of Engineering, EESC
University of São Paulo, USP
São Carlos, Brazil
rodrigoibarros@usp.br, moisesdavi@usp.br
jcarlos@sc.usp.br

Daniel Motter
Center of Engineering and Exact Sciences
Western Paraná State University, UNIOESTE
Foz do Iguaçu, Brazil
daniel.motter@unioeste.br

***Abstract*—Passive anti-islanding protections rely on measurements of voltage, frequency, and rate of change of frequency at the point of common coupling of the distributed generators, and their performance is impacted by the dynamic behavior of distributed generators operating under specific control modes. In this context, this paper proposes a novel heuristic-based method for setting the excitation system parameters of synchronous distributed generators using the differential evolution algorithm to enhance the performance of anti-islanding protection. The results demonstrate that the heuristic-based method achieves improved islanding detection performance compared to traditional values used to specify excitation system parameters. Furthermore, the optimized excitation system parameters do not adversely affect the transient response of the generator during fault events.**

***Index Terms*—Differential Evolution, Distributed Generation, Anti-Islanding Protection, Renewable Energy.**

ABBREVIATIONS

27/59	Under/Over Voltage Protections.
81R	Rate of Change of Frequency Protection.
81U/O	Under/Over Frequency Protections.
DE	Differential Evolution.
DG	Distributed Generator.
NDZ	Non-Detection Zone.
OF	Objective Function.
RoCoF	Rate of Change of Frequency.
SDG	Synchronous Distributed Generator.
FDZ	False Detection Zone.

This paper was supported in part by Coordination for the Improvement of Higher Education Personnel - Brazil (CAPES) - Financial Code 001, in part by National Council for Scientific and Technological Development (CNPq), in part by the São Paulo Research Foundation (FAPESP) grant number 2022/00483-0, and in part by CPFL Energia, Brazil under Grant ANEEL R&D program PD-00063-3085/2022.

NOMENCLATURE

A_T	Component of the objective function related to the actuation time of anti-islanding protections
E_S	Component of the objective function related to the dynamic performance of the synchronous distributed generator
$E_{S_V}^{i,G}$	Sum of the squared error between each sample j of the voltage signal during a single-phase fault and the pre-fault value at the generation G
$E_{S_P}^{i,G}$	Sum of the squared error between each sample j of the voltage signal during a single-phase fault and the pre-fault value at the generation G
$T_{81O}^{i,G}$,$T_{81U}^{i,G}$	Actuation time of 81O/81U protection function for the individual i at the generation G (ms)
$T_{81R}^{i,G}$	Actuation time of 81O protection function for the individual i at the generation G (ms)
V_j,P_j	Sample j of the voltage and active power signals during a single-phase fault at the point of common coupling of the synchronous distributed generator
V_{pre},P_{pre}	Pre-fault values of the voltage and active power measured at the point of common coupling of the synchronous distributed generator
C_{A_T},C_{E_S}	Weights assigned to the $A_T(\overrightarrow{X_i^G})$ and $E_S(\overrightarrow{X_i^G})$ components of the objective function
N_{A_T},N_{E_S}	Normalization constants of the $A_T(\overrightarrow{X_i^G})$ and $E_S(\overrightarrow{X_i^G})$ components of the objective function
NP	Number of vectors of the population
F, C	Scale factor and crossover constant
D	Number of dimensions of each vector
$\overrightarrow{X_i^G}$	Target vector of index i at the generation G
$\overrightarrow{V_i^G}$	Donor vector of index i at the generation G
$\overrightarrow{U_i^G}$	Trial vector of index i at the generation G

$u_{j,i}^G$,$v_{j,i}^G$,$x_{j,i}^G$	Parameter j of individual i at the generation G
V_Q	Output signal of reactive power control
V_{REF}	Voltage reference of the reactive power control
KP_Q,KI_Q	Gains of the proportiona-integrative controller
T_C,T_B	Time constants of the lead-lag filter
K_A,T_A	Gain and time constant of the voltage regulator
K_E,T_E	Gain and time constant of the exciter model
K_F,T_F	Gain and time constant of the negative feedback

I. Introduction

A. Motivation and Incitement

An islanding event occurs when a portion of the electrical system, including Distributed Generators (DGs) and consumer units, becomes disconnected from the main grid and remains energized without the knowledge or permission of the utility [1]. Grid codes recommend the fast disconnection of DGs to minimize the negative impacts of the islanded operation on the electrical system [1]. To achieve this, local passive anti-islanding protections are commonly used, which act by measuring an electrical quantity at the point of common coupling of the DG [2], [3]. The most common passive protection functions are the under/over frequency (81U/O), rate of change of frequency (81R, RoCoF), and under/over voltage (27/59).

However, in operating conditions with low active and/or reactive power imbalance, passive techniques may not detect islanding in an adequate time interval, leading to Non-Detection Zones (NDZs) [4]–[7]. In the past, sensitive settings have been used for these protections to reduce NDZs and ensure a fast disconnection of the DGs in the event of an islanding. Still, in a scenario with high penetration of distributed generation, more relaxed settings are needed to ensure the dependability and security of the protection scheme [8], *i.e.*, it acts for islanding events and does not act for other events, such as short circuits, load switching, among others. The IEEE 1547-2018 standard [1] also presents the ride-through requirements, which determine the frequency, voltage, and RoCoF values for which the DG must remain connected to the electrical grid.

Thus, new solutions must be proposed to reduce the NDZs of passive anti-islanding protections, while satisfying the ride-through requirements simultaneously. In [9], the authors show that when the excitation system of the Synchronous Distributed Generator (SDG) is configured to control the terminal voltage, the 27/59 protection function has a large NDZ, which makes its application for islanding detection unfeasible. Additionally, the NDZ of the 81U/O protection function may be larger, depending on the operating conditions, compared to scenarios in which the excitation system is configured to control reactive power. Since the performance of passive anti-islanding protections is influenced by the control mode of the SDG excitation system, the proper setting of the control parameters may also affect the protection's performance.

B. Literature Review

In the literature, several papers have applied heuristic-based methods to identify and/or optimize the parameters of the excitation system model. However, optimizing the model gains and time constants in the context of islanding detection has not been investigated so far. In [10] and [11], the particle swarm optimization algorithm is used to identify the parameters of the excitation system model by comparing the real system response to a reference signal. In [12] and [13], methodologies that employ genetic algorithms for the same purpose are developed. Finally, in [14], modifications are made to the mutation and crossover operators of the Differential Evolution (DE) algorithm to propose an algorithm that presents better convergence when applied to the problem of identifying the parameters of the excitation system.

C. Contribution and Paper Organization

In this context, this paper proposes a novel heuristic-based method for setting the excitation system parameters of SDGs using the DE algorithm to enhance the performance of anti-islanding protection. This algorithm aims to minimize an objective function (OF) that considers the actuation time of anti-islanding protections (81U/O, 81R) and the dynamic performance of the SDGs after the occurrence of a fault at the point of common coupling (PCC) to guarantee a proper dynamic response of the SDG control. Simulations of islanding and fault events were performed in several operating conditions in a distribution system to validate the effectiveness of the proposed method. The results revealed that optimizing the excitation system parameters improved the performance of the anti-islanding protections, reducing their NDZ without negatively affecting the transient response after a short circuit at the PCC of the SDG. In addition, once only passive techniques are employed to disconnect the SDG, there is no impact on the power quality.

Based on this context and recognizing the need for studies on this topic, the main contributions of this paper are:

- A novel heuristic-based method for setting the excitation system parameters of SDGs to enhance the performance of passive anti-islanding protections 81U/O and 81R;
- Proposal of an OF that minimizes the actuation time of existing passive anti-islanding protections, without the need for new settings and not affecting the protection security in the occurrence of faults in the distribution grid;
- The effectiveness of the proposed method is validated by the simulations of islanding and fault events in a distribution system, analyzing frequency and RoCoF signals in the time domain, in addition to the NDZ and False Detection Zone (FDZ) of passive protections;
- The proposed technique's impact on the SDG's overall performance was evaluated through the analysis of the active power and voltage signals at the SDG's terminal.

The paper is structured as follows: in Section 2 the OF, simulation method, and the DE heuristic are described; Section 3 presents the results; and Section 4 presents the conclusions.

II. Methodology

A. Proposed Objective Function

In this paper, the proposed method aims to minimize the actuation time of the anti-islanding protections, as well as guarantee a good performance of the excitation system model during disturbances in the electrical system. Thus, to calculate the OF, it is necessary to perform electromagnetic transient simulations of islanding events to obtain the trip signals of the passive anti-islanding protections and short circuit events, which will return the voltage and active power signals at the PCC of the SDG.

The first component of the OF, referring to the performance of the anti-islanding protections, is presented in (1). Considering the excitation system model is set with the parameters of a vector $\overrightarrow{X_i^G}$, in which each element represents the value of a gain or a time constant, the actuation time of the anti-islanding protections 81O, 81U, and 81R are represented by the variables $T_{81O}^{i,G}$, $T_{81U}^{i,G}$, and $T_{81R}^{i,G}$, respectively. The equation considers only the actuation time of the anti-islanding protection with the best performance (shortest actuation time).

$$A_T(\overrightarrow{X_i^G}) = min\left(T_{81O}^{i,G}, T_{81U}^{i,G}, T_{81R}^{i,G}\right) \tag{1}$$

The second component of the OF is described in (2), being related to the dynamic performance of the SDG after a short circuit at the PCC of the SDG. The variable $E_{S_V}^{i,G}$, presented in (3), is the sum of the squared error between each sample j of the voltage signal (V_j) during a single-phase fault at the PCC of the SDG and the pre-fault reference value (V_{pre}). Thus, the error for the three-phase voltage is calculated, and only the phase with the highest error is considered. Likewise, the variable $E_{S_P}^{i,G}$, described in (4), is the sum of the squared error between each sample j of the SDG active power signal (P_j) over time during a single-phase fault at the PCC and the pre-fault reference value P_{pre}. Including voltage and active power fluctuations in the problem formulation ensures that the SDG adequately controls the terminal voltage and active power injection, even after a disturbance in the electrical grid.

$$E_S(\overrightarrow{X_i^G}) = E_{S_V}^{i,G} + E_{S_P}^{i,G} \tag{2}$$

$$E_{S_V}^{i,G} = \sum \left(V_j - V_{pre}\right)^2 ; j = 1 \text{ to total of samples} \tag{3}$$

$$E_{S_P}^{i,G} = \sum \left(P_j - P_{pre}\right)^2 ; j = 1 \text{ to total of samples} \tag{4}$$

Therefore, the complete OF is described in (5). The parameters C_{A_T} and C_{E_S} indicate the weights assigned to each component of the OF, being constants with values between 0 and 1, and their sum must be equal to unity $(C_{A_T} + C_{E_S} = 1)$. The constants N_{A_T} and N_{E_S} normalize the components $A_T(\overrightarrow{X_i^G})$ and $E_S(\overrightarrow{X_i^G})$, respectively, ensuring that both parts have the same order of magnitude. The constant N_{A_T} is the best OF value after executing the DE algorithm with C_{A_T} equal to 1 and C_{E_S} equal to 0. Similarly, the constant N_{E_S} corresponds to the best OF value obtained after executing the DE algorithm with C_{A_T} equal to 0 and C_{E_S} equal to 1.

$$\min f(\overrightarrow{X_i^G}) = C_{A_T} \cdot \frac{A_T(\overrightarrow{X_i^G})}{N_{A_T}} + C_{E_S} \cdot \frac{E_S(\overrightarrow{X_i^G})}{N_{E_S}} \tag{5}$$

Finally, penalties are considered to prevent the algorithm from converging to infeasible solutions. In (5), a penalty is added to the OF if the signals of frequency, voltage (phases A, B, and C), active power, or reactive power of the SDG are not in steady-state moments before the simulation of the islanding or short circuit events. A penalty is also inserted if the active and reactive power exported by the SDG are outside the reference values defined in the control loops. Additionally, in (1), a constant value is added to the actuation time of the anti-islanding protections that do not act properly during islanding events. The OF calculation procedure is summarized in Algorithm 1.

Algorithm 1 Algorithm to calculate the OF and perform the selection step of the DE algorithm.

1: **for** each trial and target vector **do**
2: Perform the islanding simulation and calculate (1) based on the anti-islanding protections actuation times
3: Perform the short circuit simulation and calculate (2) based on voltage and active power oscillations
4: Calculate (5) and chose the best solution
5: **end for**

B. Differential Evolution Algorithm

The DE heuristic is a method used to minimize functions in the continuous space [15]–[17]. The algorithm is divided into the following steps: initialization, mutation, crossover, and selection. This heuristic was chosen because of the need for only two control parameters: the scale factor F, which controls the amplification of the difference vector in the mutation operator, and the crossover constant C [14].

During the initialization process, an initial population is randomly created, composed of NP vectors (called target vectors) with a dimension D [16], [17]. In the problem of setting the parameters of the excitation system of SDGs, each vector of the population is a group of parameters of the excitation system (composed of gains and time constants), which are generated using a uniform distribution limited by the maximum and minimum feasible values for each parameter. To represent a D-dimension target vector of index i at the generation G, the notation (6) may be used, in which $x_{1,i}^G, x_{2,i}^G, x_{3,i}^G, ..., x_{D,i}^G$ represents each parameter of the excitation system.

$$\overrightarrow{X_i^G} = \left[x_{1,i}^G, x_{2,i}^G, x_{3,i}^G, ..., x_{D,i}^G\right] ; i = 1, 2, ..., NP \tag{6}$$

The mutation process involves recombining the existing target vectors to create new solutions [16], [17]. The operation showed in (7) consists of randomly selecting three target vectors ($\overrightarrow{X_{r1}^G}$, $\overrightarrow{X_{r2}^G}$ and $\overrightarrow{X_{r1}^G}$), subtracting two of them and multiplying the result by the scale factor F. Finally, the resulting vector is added to the third one, creating a donor vector $\overrightarrow{V_i^G}$.

$$\overrightarrow{V_i^G} = \overrightarrow{X_{r1}^G} + F(\overrightarrow{X_{r2}^G} - \overrightarrow{X_{r3}^G}) \tag{7}$$

In the crossover operation, the target and donor vectors exchange parameters to create a new population of trial vectors, represented by (8) [16], [17]. The procedure is described in (9) and is performed for all D parameters. If a randomly generated value (between 0 and 1) is minor than the crossover constant C (which has a fixed value between 0 and 1), the trial vector receives the donor vector parameter. Otherwise, the target vector parameter is assigned. A new trial population is created after performing this operation on all NP vectors from both the target and donor populations.

$$\overrightarrow{U_i^G} = \left[u_{1,i}^G, u_{2,i}^G, u_{3,i}^G, ..., u_{D,i}^G\right]; i = 1, 2, ..., NP \tag{8}$$

$$u_{j,i}^G = \begin{cases} v_{j,i}^G & \text{if } rand_j \leq C \\ x_{j,i}^G & \text{otherwise} \end{cases}; j = 1, 2, ..., D \tag{9}$$

Finally, in the selection operation, the value of the OF is calculated for each vector of the target and trial populations, selecting the vector with the best performance. The resulting population will be the next generation's target population, and these steps repeat until the convergence criterion is satisfied [16], [17].

C. Complete Optimization Algorithm

The steps for applying the complete DE algorithm are:

Step 1: Define the settings of the anti-islanding protections, maximum time interval for islanding detection, characteristics of the short circuit event (fault resistance and clearance time), and the load/generation level for the dynamic simulations. Also, define the control parameters F, C, population size, and maximum number of generations for the DE heuristic;

Step 2: Estimate the normalization constants N_{A_T} and N_{E_S};

- To determine N_{A_T}, execute the DE heuristic using only (1) as the OF. Store the OF value of the best solution;
- To determine N_{E_S}, execute the DE heuristic using only (2) as the OF. Store the OF value of the best solution.

Step 3: Set values between 0 and 1 to the constants C_{A_T} and C_{E_S}, and execute the DE heuristic adopting (5) as OF.

III. Application and Results

This section presents the application of the proposed method in a modified version of the IEEE 34-bus test feeder [18] modeled in ATP, which diagram is presented in Fig. 1. The main modifications include the connection of a Diesel SDG in bus 848. Additionally, the voltage regulator in bus 852 was modeled as an on-load tap changer, the capacitor bank in bus 844 was disconnected, and the loads were modeled as constant impedance [4]. The islanding event is caused by the opening of switch SW1.

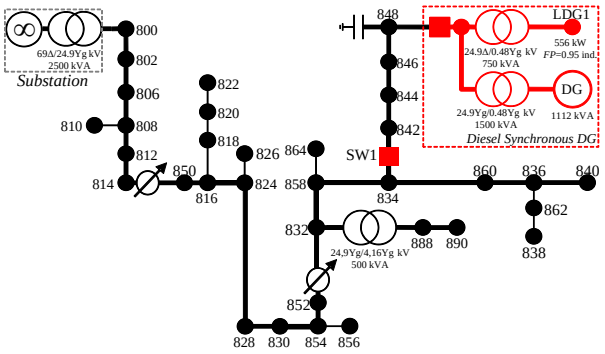

Fig. 1. Modified IEEE 34-bus test feeder. Based on [4].

The voltage control model of the excitation system of the SDG is type IEEE DC1C [19]. The reactive power control is based on the IEEE var type II model, which generates an output signal V_Q. This signal is added to the voltage reference V_{REF} and used as input to the voltage control [19]. The complete model of the excitation system is presented in Fig. 2.

The parameters KP_Q and KI_Q are the PI controller gains of the reactive power control loop. In the voltage control loop, the parameters T_C and T_B are the time constants of the lead-lag filter, T_A is the time constant, and K_A is the voltage regulator gain, while K_E and T_E are related to the exciter model. Finally, K_F and T_F are responsible for stabilizing the control model through negative feedback [19]. In addition, the speed regulator model was based on [4]. All SDG parameters are detailed in the Appendix.

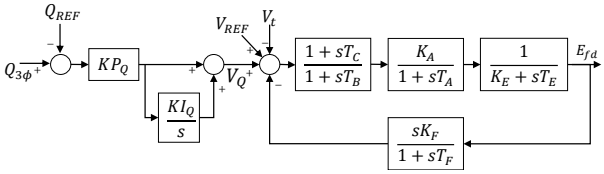

Fig. 2. Excitation system model.

A. Application of the Heuristic Method

The settings of the anti-islanding protections are presented in Tab. I and were defined respecting the ride-through requirements presented in the IEEE standard 1547-2018 [1].

The islanding event simulated to calculate the A_T portion of the OF occurs by the opening of switch SW1. In addition, the short circuit event simulated to calculate the E_S portion of

TABLE I
ANTI-ISLANDING PROTECTIONS SETTINGS.

ANSI	Pickup	Time Delay
81O	62 Hz	0.1 s
81U	57 Hz	0.1 s
81R	3 Hz/s	0 s

the OF is a single-phase short circuit at the point of common coupling of the SDG (bus 848) with a fault resistance of 25 Ω and clearance time of 500 ms. In both events, the SDG generates 0.69 p.u. of active power and 0.16 p.u. of reactive power, resulting in an operative scenario with active and reactive power imbalance of 0.27 p.u. and 0.30 p.u., respectively.

The parameters of the excitation system model are shown in Tab. II, highlighting the variation range of each parameter. According to the IEEE standard 421.5-2016 [19], T_A, K_E, and T_E are related to the excitation system model and were kept fixed. The variation ranges of the PI controller gains were defined based on previous simulations. In addition, the maximum and minimum limits defined for the parameters T_C, T_B, K_A, K_F, and T_F were defined to allow a wide variation around the base values presented in [19].

TABLE II
PARAMETERS OF THE EXCITATION SYSTEM MODEL.

$0.1 \leq KP_Q \leq 0.25$ p.u.	$0.0001 \leq K_F \leq 1$ p.u.
$0.1 \leq KI_Q \leq 5$ p.u.	$0.01 \leq T_F \leq 10$ s
$0 \leq T_B \leq 0.01$ s	$T_A = 0.06$ s
$0 \leq T_C \leq 0.01$ s	$K_E = 1$ p.u.
$10 \leq K_A \leq 850$ p.u.	$T_E = 0.46$ s

The control parameters used in the DE heuristic were defined based on several simulations and are:

- Dimensions (D): 7 (variables are the parameters KP_Q, KI_Q, T_B, T_C, K_A, K_F and T_F);
- Population size (NP): 15;
- Converge criteria: maximum of 30 generations;
- Scale factor (F): 1.2 in the first five generations, 0.8 in the last ten generations, and 1.0 in other generations;
- Crossover constant (C): 0.6.

During the execution of the DE algorithm, the OF is calculated for two populations in the selection process: trial and target population. In a generation, two electromagnetic transient simulations are performed for each individual of both populations. Considering that, in this paper, it was defined a population size of 15 individuals and the convergence criteria is a maximum of 30 generations, it is necessary to perform 1800 electromagnetic transient simulations to run the optimization algorithm. In addition, other 1800 simulations are needed to calculate the normalization constants that are part of the objective function, totaling 3600 simulations.

The first step of the proposed algorithm is the estimation of the normalization constants N_{A_T} and N_{E_S}. The values of A_T and E_S in the OF are normalized so that both have the same order of magnitude. Thus, the influence of each function on the final value of the OF (when the weights C_{A_T} and C_{E_S} are equal) will be the same, allowing a fair analysis. The value of the normalization constant is the fitness of the best solution in each execution, which in this case study resulted in $N_{E_S} = 900.0$ p.u. and $N_{A_T} = 130.72$ p.u.

In order to obtain an overview of the impact of the OF weights on the performance of anti-islanding protections, five sets of solutions were obtained by varying the weights C_{A_T} and C_{E_S} of the OF:

- Set 1: $C_{A_T} = 0$ and $C_{E_S} = 1$;
- Set 2: $C_{A_T} = 0.25$ and $C_{E_S} = 0.75$;
- Set 3: $C_{A_T} = 0.5$ and $C_{E_S} = 0.5$;
- Set 4: $C_{A_T} = 0.75$ and $C_{E_S} = 0.25$;
- Set 5: $C_{A_T} = 1$ and $C_{E_S} = 0$.

The values of the parameters of the SDG excitation system for each solution are presented in Tab. III. In addition, the actuation times of the anti-islanding for these solutions after an islanding event with an active power imbalance of 0.27 p.u. and reactive power imbalance of 0.30 p.u. (same operating condition defined as input data for the heuristic method) are presented in Tab. IV. The acting time of the function 81R was less than 150 ms for all solutions. In addition, solutions Set 1 and Set 2 presented the highest acting time for this function, while solution Set 5 resulted in the best performance. Also, considering the combined function 81U/O, the islanding event was not detected within the maximum detection time of 2 s only for solution Set 2.

TABLE III
OPTIMIZED PARAMETERS OF THE EXCITATION SYSTEM.

Parameters	Set 1	Set 2	Set 3	Set 4	Set 5
KP_Q (p.u.)	0.1737	0.1248	0.25	0.25	0.25
KI_Q (p.u.)	5	5	5	5	0.305
T_B (s)	0.0033	0.01	0.01	0.0065	0.0036
T_C (s)	0.0014	0.01	0.0027	0.01	0.01
K_A (p.u.)	565	850	850	10	46
K_F (p.u.)	0.328	1	1	0.865	0.755
T_F (s)	2.5183	8.31	10.0	2.7663	10.0

TABLE IV
ANTI-ISLANDING PROTECTIONS ACTUATION TIME AFTER THE OPTIMIZATION.

	Set 1	Set 2	Set 3	Set 4	Set 5
81O (ms)	1686	-	1365	14301	-
81U (ms)	-	-	-	850.46	1403
81R (ms)	147.38	148.42	139.05	136.97	130.72

In order to obtain an overview of the impact of the OF weights on the frequency and RoCoF oscillations, Fig. 3a and Fig. 3b present the frequency and RoCoF signals, respectively, in the time-domain after an islanding event for the five solutions previously presented in Tab. III.

From Fig. 3a, it is noted that for the solutions Set 1 and Set 2, in which the weight given to the minimization of the anti-islanding protection actuation time is null and 0.25, respectively, the frequency signal presents the smaller oscillations around the 60 Hz reference, which results in higher acting times for the islanding protections. Therefore, a more

sensitive setting is necessary to guarantee the performance of the 81U/O protection function. The frequency oscillation is more severe for the other solutions, reaching values below 55 Hz for solution Set 5 and above 65 Hz for solutions Set 3 and Set 4, allowing more relaxed settings.

From the RoCoF signals presented in Fig. 3b, despite function 81R having the shortest actuation time when adopting the parameters of the solution Set 5, the RoCoF signal drops to a minimum of -5 Hz/s. On the other hand, for solution Set 3, the RoCoF signal raises to 10 Hz/s, indicating that if a more relaxed setting was adopted (or a longer time delay), these excitation system parameters would still guarantee the disconnection of the SDG after the islanding event.

Aiming to evaluate the dynamic performance of the SDG for the five solutions, Fig. 4 shows the voltage and active power signals during and after a short circuit event with a duration of 500 ms at the PCC of the SDG. The difference between the voltage and active power oscillations for each solution is not significant. Also, even with a voltage drop to values below 0.60 p.u. during the short circuit and a large oscillation of the SDG active power, it is observed that the system is able to restore the balance after the extinction of the short circuit. Thus, it is concluded that the best strategy is to adopt weights equal to 0.5 for calculating the OF, ensuring compliance between islanding detection and dynamic performance of the SDG for other disturbances in the electrical grid.

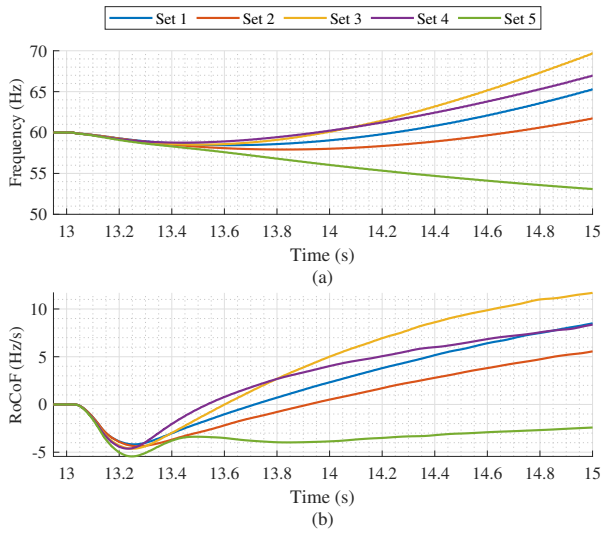

Fig. 3. Comparison of the signals of (a) frequency and (b) RoCoF after an islanding event.

B. Comparison With Standard Settings

This section is dedicated to comparing the performance of the anti-islanding protections when the excitation system of the SDG is modeled with the set of parameters obtained by the proposed heuristic and with standard parameters available in the literature. Thus, the Set 3 solution is compared with the gains presented in the IEEE standard 421.5-2016 [19] and described in Tab. V. The gains KP_Q and KI_Q are not included in the standard and were adjusted using the parameters available in [4].

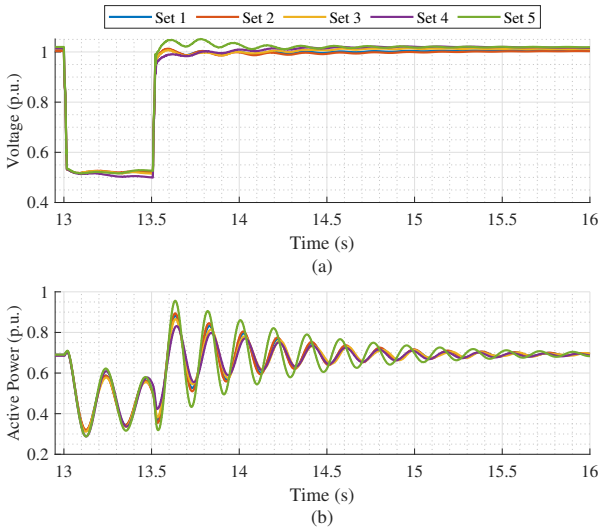

Fig. 4. Comparison of the signals of (a) voltage and (b) active power after a short circuit event.

TABLE V
STANDARD PARAMETERS OF THE EXCITATION SYSTEM MODEL. BASED IN [4], [19].

KP_Q	0.25 p.u.	K_F	0.1 p.u.
KI_Q	0.5 p.u.	T_F	1 s
T_B	0 s	T_A	0.06 s
T_C	0 s	K_E	1 p.u.
K_A	46 p.u.	T_E	0.46 s

The frequency and RoCoF signals after an islanding event in the same operative scenario of the previous sections are presented in Fig. 5. By adopting the parameters set out in the IEEE 421.5-2016 standard, the frequency (Fig. 5a) does not exceed the range of 55 Hz, while in the scenarios in which the excitation system is modeled with the parameters obtained by the heuristic, the frequency deviates to values close to 70 Hz. Likewise, the RoCoF signal (Fig. 5b) oscillates less when using the parameters of the IEEE 421.5-2016 standard so that the protection would not be sensitized if a setting of 5 Hz/s was adopted.

In addition, by the voltage and active power signals when a phase-to-ground short circuit event occurs at the point of common coupling of the SDG (Fig. 6), it is noted that when adopting the optimized parameters, the voltage and active power oscillates less after the extinction of the disturbance. Therefore, in addition to guaranteeing higher oscillations after an islanding, the proposed method guarantees a better performance of the SDG when subjected to a short circuit.

C. Non-Detection Zone and False Detection Zone Analysis

To highlight the improved performance of the anti-islanding protections achieved with the proposed method, Fig. 7 presents the NDZs of 81R and 81U/O functions when the SDG's excitation system is modeled with the parameters of solution

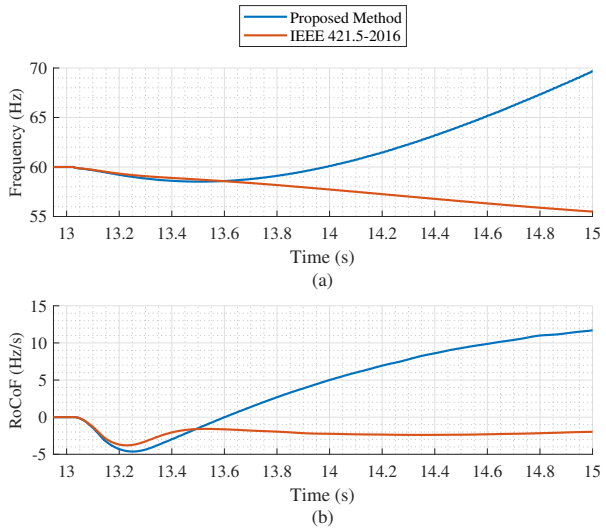

Fig. 5. Comparison of the signals of (a) frequency and (b) RoCoF after an islanding event.

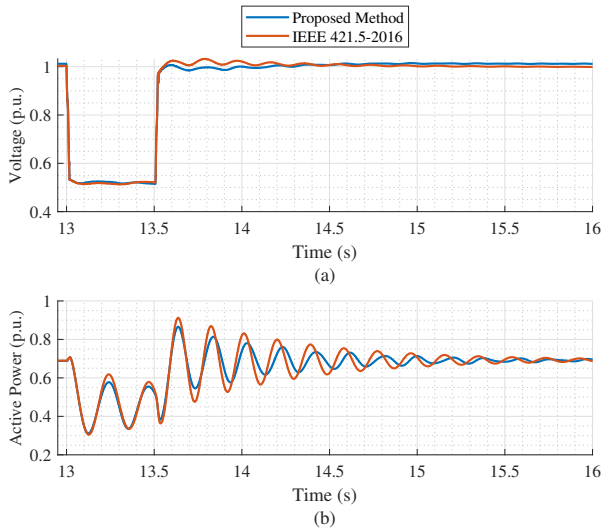

Fig. 6. Comparison of the signals of (a) voltage and (b) active power after a short circuit event.

Set 3 (Fig. 7a and Fig. 7b, respectively) and when the excitation system is modeled with the parameters of the IEEE 451.5-2016 standard (Fig. 7c and Fig. 7d, respectively). The NDZ of 81R (Fig. 7a) and 81U/O (Fig. 7b) functions after the simulations with the optimized parameters of the excitation system are composed of only one operative point with active and reactive power imbalance close to zero. On the other hand, when adopting the parameters of the IEEE 524.5-2016 standard, the NDZs of both functions are much higher, once 81R (Fig. 7c) and 81U/O (Fig. 7d) do not act properly in 12 and 10 operative points.

In addition, Tab. VI presents the FDZ of passive anti-islanding methods. The results were obtained by applying the methodology described in [20], and the FDZ index represents the percentage of short circuit events (from 300 events) in which the anti-islanding protection acted incorrectly. When the excitation system is set with the parameters of the IEEE 451.5-2016 standard, there is no FDZ for 81U/O protection functions. In addition, the 81R protection function has a large FDZ if an instantaneous setting is adopted, but it is eliminated by adopting a time delay of 100 ms. Also, when the SDG's excitation system is modeled with the parameters of solution Set 3, the FDZ of the passive techniques varies less than 1%. Therefore, the optimization can reduce the NDZ of passive techniques without negatively affecting the FDZ.

TABLE VI
FDZ OF PASSIVE ANTI-ISLANDING PROTECTIONS.

ANSI	Setting	Time Delay	FDZ(%)	
			IEEE	Set 3
81U/O	57/62 Hz	0.1 s	0	0
81R	3.0 Hz/s	0 s	99.19	98.37
81R	3.0 Hz/s	0.1 s	0	0.41

IV. CONCLUSIONS

This paper presented the use of the DE heuristic to set the parameters of the excitation system of a SDG from the perspective of the anti-islanding protection scheme performance. In this approach, the OF of the problem seeks to minimize the actuation time of the anti-islanding protection scheme, also considering the SDG's behavior when subjected to a single-phase short circuit at the point of common coupling. The results demonstrate that the heuristic-based method reduced the NDZs of passive anti-islanding protections compared to traditional values used for specifying excitation system parameters, and do not adversely affected the FDZ of passive techniques and the transient response of the generator during fault events. In conclusion, by considering specific requirements and utilizing a heuristic optimization algorithm, this methodology enables the identification of optimal parameter values that improve the dependability of islanding protections when adopting settings based on the ride-through requirements. The main topics for the continuation of this research include conducting simulations in closed-loop and real-time to enhance the robustness of the findings and comparing the performance of the DE algorithm with other heuristic methods.

APPENDIX
SYNCHRONOUS DISTRIBUTED GENERATOR PARAMETERS

The parameters of SDG connected at bus 848 are: $S = 1.112\ MVA$; $V = 0.480\ kV_{ll}$; $f = 60\ Hz$; $N = 1200\ rpm$; $H = 0.4182\ s$; $R_a = 0.027 p.u.$; $X_L = 0.1 p.u.$; $X_d = 2.081 p.u.$; $X_q = 1.144 p.u.$; $X_d^{'} = 0.295 p.u.$; $X_q^{'} = 0.2797 p.u.$; $X_d^{"} = 0.193 p.u.$; $X_q^{"} = 0.183 p.u.$; $T_{d0}^{'} = 3.007 s$; $T_{q0}^{'} = 1.592 s$; $T_{d0}^{"} = 0.0153 s$; $T_{q0}^{"} = 0.0081 s$; $X_{CAN} = 0.1 p.u.$. The SDG were modeled considering the following parameters for the speed governor: $K_{control} = 20$; $K = 80$; $T_d = 0.0025 s$; $T_1 = 0.01 s$; $T_2 = 0.02 s$; $T_3 = 0.2 s$; $T_4 = 0.25 s$; $T_5 = 0.39 s$; $T_6 = 0.009 s$.

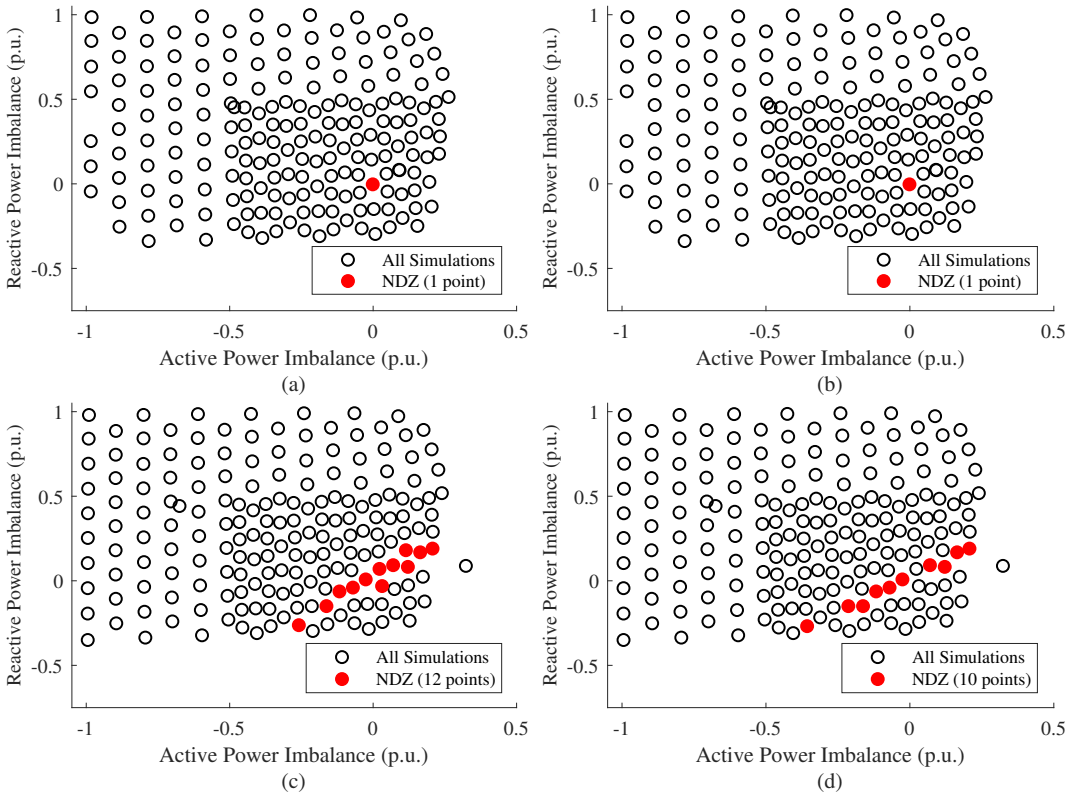

Fig. 7. NDZs of 81R (a) and 81U/O (b) functions when the SDG excitation system is modeled with the parameters of solution Set 3, and NDZ of 81R (c) and 81U/O (d) functions when the SDG excitation system is modeled with the parameters of IEEE standard 421.5-2016.

REFERENCES

[1] *IEEE 1547-2018 - IEEE Standard for Interconnection and Interoperability of Distributed Energy Resources with Associated Electric Power Systems Interfaces*, New York, NY, 2018.

[2] C. Li, C. Cao, Y. Cao, Y. Kuang, L. Zeng, and B. Fang, "A review of islanding detection methods for microgrid," *Renewable and Sustainable Energy Reviews*, vol. 35, no. C, pp. 211–220, 2014.

[3] P. Mahat, Z. Chen, and B. Bak-Jensen, "Review of islanding detection methods for distributed generation," in *2008 Third International Conference on Electric Utility Deregulation and Restructuring and Power Technologies*, 2008, pp. 2743–2748.

[4] D. Motter and J. C. de Melo Vieira, "The setting map methodology for adjusting the dg anti-islanding protection considering multiple events," *IEEE Transactions on Power Delivery*, vol. 33, no. 6, pp. 2755–2764, 2018.

[5] D. Salles, W. Freitas, J. C. M. Vieira, and W. Xu, "Nondetection index of anti-islanding passive protection of synchronous distributed generators," *IEEE Transactions on Power Delivery*, vol. 27, no. 3, pp. 1509–1518, 2012.

[6] D. Mlakić, H. R. Baghaee, and S. Nikolovski, "Gibbs phenomenon-based hybrid islanding detection strategy for vsc-based microgrids using frequency shift, thd_U , and rms_U," *IEEE Transactions on Smart Grid*, vol. 10, no. 5, pp. 5479–5491, 2019.

[7] ——, "A novel anfis-based islanding detection for inverter-interfaced microgrids," *IEEE Transactions on Smart Grid*, vol. 10, no. 4, pp. 4411–4424, 2019.

[8] J. L. Blackburn, *Protective relaying: Principles and applications*. CRC Press Inc, 2014.

[9] J. C. M. Vieira, W. Freitas, W. Xu, and A. Morelato, "An investigation on the nondetection zones of synchronous distributed generation anti-islanding protection," *IEEE Transactions on Power Delivery*, vol. 23, no. 2, pp. 593–600, 2008.

[10] S. Kittiwattanaphon, W. Wangdee, and S. Katithummarugs, "Generator excitation system parameter identification and tuning by using pso," in *2019 7th International Electrical Engineering Congress (iEECON)*, 2019, pp. 1–4.

[11] P. Yu and J. Zhang, "Parameter identification of excitation system based on field data and pso," in *2010 International Conference on E-Product E-Service and E-Entertainment*, 2010, pp. 1–4.

[12] J. Q. Puma, "Parameters identification of excitation system models using genetic algorithms," *IET Generation, Transmission & Distribution*, vol. 2, pp. 456–467(11), 2008.

[13] S. Feng, X. Jianbo, W. Guoping, and X. Yong-hong, "Study of brushless excitation system parameters estimation based on improved genetic algorithm," in *2008 Third International Conference on Electric Utility Deregulation and Restructuring and Power Technologies*, 2008, pp. 915–919.

[14] N. Li, Y. Liu, and B. Geng, "Research on parameter identification method of generator excitation system based on differential evolution algorithm," *IOP Conference Series: Materials Science and Engineering*, vol. 752, no. 1, p. 012017, 2020.

[15] R. Stom and K. Price, "Differential evolution-a simple and efficient adaptive scheme for global optimization over continuous spaces," *Technical Repan, TR-95.012, ICSI*, 1995.

[16] Bilal, M. Pant, H. Zaheer, L. Garcia-Hernandez, and A. Abraham, "Differential evolution: A review of more than two decades of research," *Engineering Applications of Artificial Intelligence*, vol. 90, p. 103479, 2020.

[17] S. Das and P. N. Suganthan, "Differential evolution: A survey of the state-of-the-art," *IEEE Transactions on Evolutionary Computation*, vol. 15, no. 1, pp. 4–31, 2011.

[18] IEEE, "IEEE distribution test feeders. radial distribution test feeders," 2021. [Online]. Available: https://site.ieee.org/pes-testfeeders/resources/

[19] "IEEE recommended practice for excitation system models for power system stability studies," *IEEE Std 421.5-2016 (Revision of IEEE Std 421.5-2005)*, pp. 1–207, 2016.

[20] R. de Barros Iscuissati, D. Motter, and J. C. M. Vieira, "Probabilistic analysis of dg anti-islanding protection security against momentary short-circuits in distribution grids," in *2021 Workshop on Communication Networks and Power Systems (WCNPS)*, 2021, pp. 1–6.